Acta Crystallographica Section D
Biological Crystallography
ISSN 0907-4449

Crystallization of the effector-binding domains of BenM and CatM, LysR-type transcriptional regulators from *Acinetobacter* sp. ADP1

Todd Clark,[a] Sandra Haddad,[a] Ellen Neidle[a] and Cory Momany[b]*

[a]Department of Microbiology, University of Georgia, Athens, GA, USA, and [b]Department of Pharmaceutical and Biomedical Sciences, University of Georgia, Athens, GA, USA

Correspondence e-mail: cmomany@mail.rx.uga.edu

Received 28 August 2003
Accepted 29 September 2003

BenM, a member of the LysR-type family of transcriptional regulators, controls genes for benzoate degradation in the Gram-negative bacterium *Acinetobacter* sp. strain ADP1. Recent studies show that BenM activates *benABCDE* expression synergistically in response to two effector ligands: *cis*,*cis*-muconate (CCM) and benzoate. As an initial step in investigating the structural basis of dual effector response, the effector-binding domain of BenM (BenM-EBD) was crystallized by the microbatch-under-oil technique with conditions optimized from high-throughput screens performed by the Hauptman–Woodward Institute. Data-collection quality crystals of BenM-EBD belonged to space group $P2_12_12_1$, diffracted to 2.3 Å and had unit-cell parameters a = 65.64, b = 66.34, c = 117.46 Å. The influence of effector ligands on crystal formation was also evaluated. The presence of benzoate or CCM impaired the formation of crystals. The presence of both effectors together resulted in a dramatic decrease in the production of crystals. The effector-binding domain of CatM, a homolog of BenM, was also crystallized.

1. Introduction

BenM controls the expression of multiple genes involved in aromatic compound degradation by the soil bacterium *Acinetobacter* sp. strain ADP1 (Brzostowicz *et al.*, 2003; Clark *et al.*, 2002; Collier *et al.*, 1998). BenM belongs to a large and diverse family of homologous prokaryotic regulators, the LysR-type transcriptional regulators (LTTRs; Henikoff *et al.*, 1988; Schell, 1993). As a representative member of this family, BenM is a good candidate for atomic level structural studies. Of particular interest is the ability of BenM to activate transcription synergistically with two different compounds. This novel feature was discovered during investigations of BenM-regulated *benA* gene expression (Bundy *et al.*, 2002). Benzoate and one of its catabolites, *cis*,*cis*-muconate (CCM), enable BenM to activate transcription *in vivo* and *in vitro*. While CCM is more effective than benzoate as a sole effector, both compounds together activate gene expression in a synergistic fashion (Bundy *et al.*, 2002; Collier *et al.*, 1998). Many transcriptional regulators respond to more than one effector. However, the combined effect of multiple compounds has not been investigated in other regulatory systems.

To understand the interactions of BenM with benzoate and CCM, our current studies focus on the effector-binding domain (EBD) of the regulator. This truncated protein, BenM-EBD, lacks the 80 amino-terminal residues of the native protein and can be purified *via* a carboxy-terminal hexahistidine tag. Fluorescence emission spectroscopy demonstrated that BenM-EBD has an affinity for effectors comparable to that of the full-length protein (Clark *et al.*, 2003). In studies of full-length BenM, the purification tag was found to have no effect on protein function *in vivo* or *in vitro* (Bundy *et al.*, 2002).

In previous studies of two LTTRs, CysB and OxyR, structures were obtained for protein fragments that lack the DNA-binding domains. The regulatory domain (residues 88–324) of CysB, which controls cysteine biosynthesis, was characterized from *Klebsiella aerogenes* (Tyrrell *et al.*, 1994, 1997). The tertiary structure of this domain is similar to a family of periplasmic binding proteins that have a Rossmann-fold topology (Quiocho, 1991). These proteins have two domains linked by a hinge that allows movement of the domains upon cofactor binding. Recently, the crystallization but not the structure of full-length CysB was reported (Verschueren *et al.*, 2001). The second atomic structure of an LTTR which has been described is a truncated fragment of OxyR from *Escherichia coli* (Choi *et al.*, 2001). OxyR regulates intracellular redox potentials by an intriguing structural rearrangement using disulfide-bond formation as the sensing switch. It shares substantial structural similarity with CysB, with a root-mean-square deviation of 1.84 Å for 167 C^{α} atoms.

BenM-EBD shares only 20 and 11% sequence identity with the comparable regions

© 2004 International Union of Crystallography
Printed in Denmark – all rights reserved

of OxyR and CysB, respectively. However, recent studies of CbnR, the first full-length LTTR structure to be characterized, suggest that a common effector-binding fold may be used throughout the family (Muraoka, Okumura, Ogawa *et al.*, 2003; Muraoka, Okumura, Uragami *et al.*, 2003). CbnR, which is 46% similar in sequence to BenM, is a plasmid-encoded regulator of chlorobenzoate degradation in *Ralstonia eutropha* (Ogawa *et al.*, 1999; Ogawa & Miyashita, 1999). It will be of interest to compare the effector-binding properties of CbnR to those of BenM, a protein which regulates benzoate degradation in a bacterium unable to degrade chlorobenzoate. Understanding the effects of halogenated substituents on the regulation of catabolic pathways is relevant to the development of successful bioremediation strategies. Structural studies of BenM will also provide a basis of comparison for the function of CatM, a second LTTR involved in benzoate degradation by *Acinetobacter* sp. strain ADP1 (Neidle *et al.*, 1989; Romero-Arroyo *et al.*, 1995). CatM and BenM are 59% identical in sequence (54% in the EBD), recognize similar DNA sequences, both respond to CCM as an effector and have overlapping functions. However, CatM does not respond to benzoate and does not respond synergistically to multiple compounds. As a first step in understanding LTTR–effector interactions, including synergistic transcriptional activation, the BenM-EBD protein was crystallized in the presence and absence of its effectors. In addition, a similarly truncated version of CatM, designated CatM-EBD, was purified and crystallized.

2. Methods

2.1. Purification of BenM-EBD and CatM-EBD

The purification of BenM-EBD will be described elsewhere (Clark *et al.*, 2003). BenM-EBD (232 amino acids, molecular weight 26 353 Da) has the added C-terminal sequence LEHHHHHH, allowing it to be purified from *Escherichia coli* in one step by metal-chelate chromatography. Fractions containing purified BenM-EBD were pooled and twice dialyzed for 4 h at 277 K in 1 l 20 m*M* Tris–HCl pH 7.9, 500 m*M* NaCl and 10% glycerol using 10 kDa molecular-weight cutoff snakeskin dialysis tubing (Pierce Biotechnology Inc.). Protein for crystallization trials was concentrated to $\geq$6 mg ml^{-1} using an Ultrafree S-10 concentrator (Millipore) and stored at 277 K until use. Benzoate (Sigma-Aldrich) and CCM (Acros Organics) solutions were prepared in 0.1 *M* NaOH, titrated to pH 7 and added at appropriate concentrations. CatM-EBD was purified from *E. coli* in a similar manner as for BenM-EBD, but dialyzed in 250 m*M* imidazole, 20 m*M* Tris–HCl pH 7.9, 500 m*M* NaCl, 1 m*M* DTT and 10% glycerol. CatM-EBD (231 amino acids, molecular weight 25 994 Da) has the same C-terminal addition as BenM-EBD.

2.2. Crystallization of BenM-EBD, CatM-EBD and effector complexes

Initial high-throughput crystallization screens (HTS) were performed at the Hauptman–Woodward Institute as microbatch-under-oil experiments at 298 K using a sitting-drop method (Luft *et al.*, 2001). Samples were purified within two weeks of the HTS run and shipped on ice. A total of 1536 conditions per sample were screened by combining 0.2 µl BenM-EBD (6 mg ml^{-1} in 20 m*M* Tris–HCl pH 7.9, 0.5 *M* NaCl, 10% glycerol) or CatM-EBD (6 mg ml^{-1} in 250 m*M* imidazole, 20 m*M* Tris–HCl pH 7.9, 0.5 *M* NaCl, 1 m*M* DTT and 10% glycerol) with 0.2 µl precipitating solution per well. Crystallizations were monitored by photography at 1, 4, 7 and 14 d. BenM-EBD samples were also evaluated with the effectors benzoate (3 m*M* initial), CCM (2.5 m*M*) and a mix of CCM and benzoate (3 and 2.5 m*M*, respectively). Subsets of these conditions were repeated in-house using 3–6 µl total volume drops, varying the temperature, precipitant-to-protein ratios and effector-to-protein ratios. Crystallization trials in-house were prepared using freshly purified protein or the same protein (stored on ice) as a corresponding HTS run. The protein samples were centrifuged briefly ($\sim$5 min) at 16 000*g* prior to setup.

2.3. X-ray analysis and data collection

Prior to data collection, BenM-EBD, CatM-EBD and BenM-EBD–effector complex crystals were briefly transferred to a cryoprotectant solution containing 30–35%(*v*/*v*) glycerol and precipitant and protein-buffer components of 10% higher concentration than the original crystallization growth condition. For the form I crystal of BenM-EBD and CatM-EBD, the cryoprotectant was 35%(*v*/*v*) glycerol, 50 m*M* ammonium sulfate, 25 m*M* sodium acetate trihydrate pH 4.6, 6.25%(*w*/*v*) PEG 4000, 9 m*M* Tris–HCl and 225 m*M* NaCl. Crystals were mounted in a cryoloop and flash-frozen in a 100 K nitrogen stream generated by an Oxford Cryojet. Native BenM-EBD and CatM-EBD data were collected in-house on a Bruker Nonius κ CCD detector mounted on an FR591 rotating-anode generator equipped with a graphite monochromator and Miracol optics operated at 45 kV and 100 mA (Cu $K\alpha$ radiation). Data-collection schemes for BenM-EBD or CatM-EBD were defined to collect complete data sets (99%) to 2.4 or 3.0 Å (CatM-EBD) with high redundancy. Each frame was exposed for 300 s with a 0.3° (0.7° for CatM-EBD) oscillation at a crystal-to-detector distance of 90 mm (56 mm for CatM) and processed with the *DENZO–SMN* package (Otwinowski & Minor, 1997). Data sets from the BenM-EBD–effector complex crystals, previously frozen in liquid Freon and shipped in a dry shipper, were collected at the SBC-CAT beamline using a wavelength of 0.97937 Å and were processed using *HKL*2000 (Otwinowski & Minor, 1997).

3. Results

BenM-EBD, like the other LTTRs that have been crystallized, is minimally soluble without NaCl and glycerol. CatM-EBD did not tolerate a reduction in the concentration of imidazole used to purify the protein. Because of the high solute concentrations used to maintain protein solubility, the microbatch-under-oil technique was most useful. HTS performed with and without effectors identified many successful crystallization conditions when visually evaluated after two weeks (>90% of the crystals appeared in one week). For BenM-EBD lacking effectors, 126 conditions of the 1536 trials yielded visible crystals. The addition of CCM decreased the number of conditions with crystals to 96. The presence of benzoate further lowered the success rate to 72 positive conditions. Significantly, only 28 conditions were identified with both benzoate and CCM present simultaneously. 49 conditions were unique to the BenM-EBD lacking effectors, 14 were unique to CCM, 18 were unique to benzoate and three were unique for benzoate and CCM. The most common crystal morphology was needles, with about 1/3 of the conditions having a thick rod-like morphology. In general, crystals that formed in the presence or absence of effectors had a similar appearance and the crystallization conditions contained common components such as acetate or citrate buffers in polyethylene glycols. Many of the crystals prepared from complexes may prove not to have ordered effectors, since the majority of crystals that formed in the presence of effectors have the same unit-cell parameters as the form I BenM-EBD crystals prepared

in the absence of effectors (Table 1). Considering the low binding constants of the effectors for BenM in the absence of DNA (CCM, K_d = 120 μ*M*; benzoate, K_d = 1100 μ*M*; Clark *et al.*, 2003), the high salt concentrations in the crystallization buffers may compete with the binding of effectors. This may be a common trend among LTTRs, since no structure of an LTTR bound to its cognate effector has yet been solved. Form I crystals of BenM-EBD lacking effector, optimal for high-resolution data collection (Fig. 1*a*), were generated at 288 K in sitting drops under paraffin oil (Chayen, 1997) by combining 4 μl BenM-EBD (≥6 mg ml^{-1}) and 1 μl of precipitating solution [0.2 *M* ammonium sulfate, 0.1 *M* sodium acetate trihydrate pH 4.6 and 25%(*w*/*v*) PEG 4000] (Hampton Research screening kit solution HR 1-20). Microdialysis against buffer containing both the protein buffer and the above precipitant in a 3:1 volume ratio also produced large BenM-EBD crystals suitable for diffraction studies. When the form I crystallization conditions were repeated in the presence of effectors (Figs. 1*b* and 1*c*), CCM appeared to have little effect, while benzoate significantly blocked crystal formation. Tryptophan fluorescence studies show that benzoate causes a conformational change, indicated by a red shift in the spectrum and lowered emission, while CCM only lowers the emission. Thus, the two effectors may cause BenM-EBD to respond differently, which may be reflected in different crystallization properties (Clark *et al.*, 2003). Alternatively, it is well established that small molecules can affect the crystallization of macromolecules independently of an associated biological function, as is the case with phenol affecting the crystallization of rhombohedral insulin (Smith & Dodson, 1992).

Table 1
Crystallization conditions and properties of BenM-EBD, CatM-EBD and effector-complex crystals.

Equal volumes (2 μl and 2 μl) of protein in protein buffer (20 m*M* Tris–HCl pH 7.9, 0.5 *M* NaCl, 10% glycerol) and precipitant were mixed together. Only the composition of the precipitant is shown. For the form I crystals, a 4:1 ratio of protein to precipitant was used. With the exception of the form I crystals, crystals were prepared only once using conditions from the HTS screens without optimization.

Complex (solution No.)	Crystallization precipitant solution	Likely space group	Unit-cell parameters (Å, °)	Diffraction limit (Å)	X-ray source
BenM-EBD (form I)	0.2 *M* $(NH_4)_2SO_4$, 0.1 *M* sodium acetate pH 4.6, 25% PEG 4K	$P2_12_12_1$	*a* = 65.64, *b* = 66.34, *c* = 117.45	2.3	Home, Cu *Kα*
CatM-EBD	0.2 *M* $(NH_4)_2SO_4$, 0.1 *M* sodium acetate pH 4.6, 25% PEG 4K	*I*222	*a* = 66.19, *b* = 75.27, *c* = 102.52	2.9	Home, Cu *Kα*
BenM-EBD + CCM (37)	0.1 *M* sodium acetate pH 4.6, 25% PEG 4K, 3 m*M* CCM	$P2_12_12_1$	*a* = 64.21, *b* = 67.03, *c* = 116.20	2.3	SBC†
BenM-EBD + CCM (347)	0. 1 *M* NaBr, 0.1 *M* CAPS pH 10, 20% PEG 20K, 3 m*M* CCM	$C222_1$	*a* = 98.81, *b* = 99.93, *c* = 187.08	3	SBC†
BenM-EBD + CCM (544)	0.1 *M* $MnSO_4$, 0.1 *M* sodium acetate pH 5, 20% PEG 8K, 3 m*M* CCM	$P2_12_12_1$	*a* = 64.49, *b* = 67.38, *c* = 116.61	2.0	SBC†
BenM-EBD + CCM (712)	0.1M K_2HPO_4, 0.1 *M* sodium citrate pH 4, 20% PEG 4K, 3 m*M* CCM	$P2_12_12_1$	*a* = 65.61, *b* = 65.25, *c* = 117.26	2.5	SBC†
BenM-EBD + benzoate (497)	0.1 *M* KBr, 0.1 *M* CAPS pH 10, 20% PEG 8K, 3 m*M* benzoate	*C*2	*a* = 289.44, *b* = 101.82, *c* = 211.90, *β* = 117.38	2.9	SBC†

† Data collected at the Structural Biology Center Collaborative Access Team (SBC-CAT) beamline, Advanced Photon Source, Argonne, IL, USA.

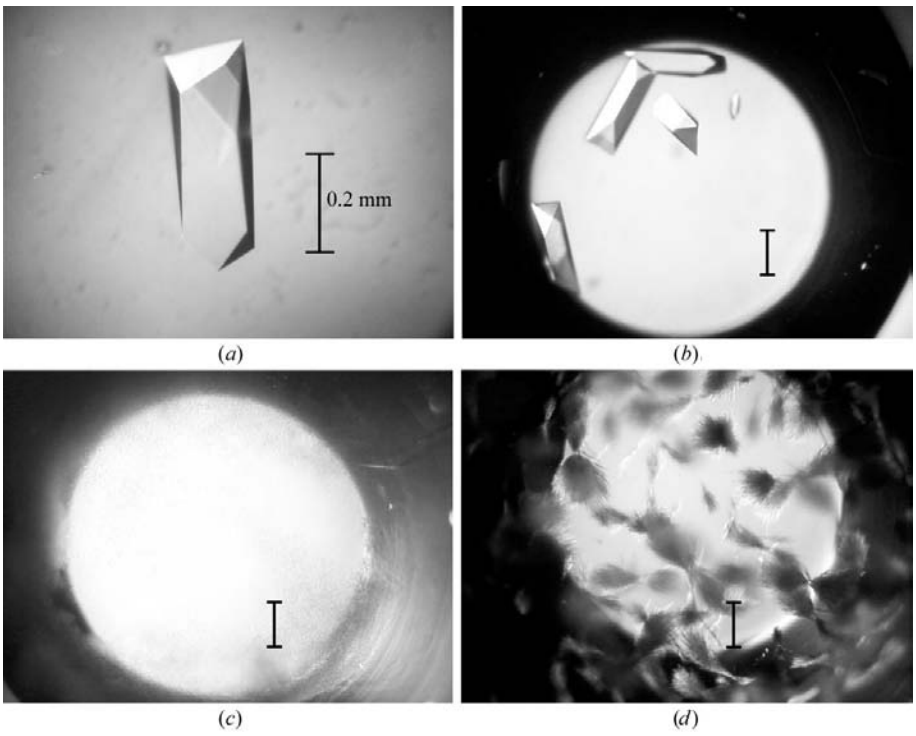

Figure 1
Influence of effectors on the formation of BenM-EBD crystals. BenM-EBD was combined with precipitant (Hampton Research kit I, solution 20) at a ratio of 4:1 at 288 K (*a*) in the absence of effectors or (*b*) in the presence of 3 m*M* CCM, (*c*) 3 m*M* benzoate or (*d*) CCM and benzoate at 3 m*M* each. The scale bar is 0.2 mm.

The diffraction data from a single crystal of BenM-EBD collected on an area detector were consistent with the space group $P2_12_12_1$, having appropriate systematic absences at *h*00, 0*k*0 and 00*l* odd. The data-collection strategy was defined to collect 99.5% of the data to 2.4 Å, but the data set was processed to 2.3 Å with an overall $R_{\rm merge}$ of 4.7% (12.8% in the 2.37–2.30 Å bin) with $\langle I/\sigma(I)\rangle$ = 50.1 (7.0 in the high resolution bin). Reflections were visible to 2.2 Å resolution. Refined unit-cell parameters were *a* = 65.64, *b* = 66.34, *c* = 117.46 Å.

CatM-EBD crystals, like most of the BenM-EBD effector-complex crystals, were thin rods, <50 μm × <50 μm × 0.2 mm. Interestingly, CatM-EBD crystallized from the same conditions as the form I crystals of BenM-EBD, although the space group and unit-cell parameters were different (*I*222 or $I2_12_12_1$; *a* = 66.19, *b* = 75.27, *c* = 102.52 Å). The conditions for growing CatM-EBD crystals are still being optimized in order to increase the crystal dimensions. The single crystal examined diffracted weakly to 2.9 Å

in-house with long exposures [R_{merge} = 20.9%, $\langle I/\sigma(I)\rangle$ = 13.8]. Because of the poor statistics, it is possible that the crystals actually belong to the lower symmetry space group *C*2. R_{merge} was only marginally lower in space group *C*2. The space-group assignment should be resolved once higher resolution data are collected.

The molecular weight of the BenM-EBD monomer (including the hexahistidine purification tag) was observed to be 26 232 Da by liquid-chromatography mass spectrometry (data not shown). BenM-EBD had an apparent molecular weight of 48 000 Da when analyzed on a standardized HiPrep Sephacryl S-200 gel-filtration column (26 × 60 cm; Amersham Pharmacia) equilibrated with 20 m*M* Tris–HCl pH 7.9, 500 m*M* NaCl and 10%(*v*/*v*) glycerol (data not shown). Taken together, these results indicate that BenM-EBD is a dimer in solution. Using the crystallographic unit-cell and space-group information and assuming two molecules per asymmetric unit, the Matthews coefficient V_M is 2.4 Å^3 Da^{-1}, which corresponds to a solvent-volume fraction of 48.9% (Matthews, 1968). Self-rotation functions were calculated using the programs *GLRF* (Tong & Rossmann, 1997) and *AMoRe* (Collaborative Computational Project, Number 4, 1994; Navaza, 1994) to identify non-crystallographic symmetry. Despite the non-crystallographic symmetry suggested by the Matthews coefficient, no strong peaks were present in the rotation-function maps (except those corresponding to the crystallographic twofold axes). Furthermore, there were no strong features in the native Patterson that would indicate a non-crystallographic twofold axis parallel to the crystallographic screw axes offset from a crystallographic axis. Since the related CysB and OxyR monomers have domains with pseudo-dyad symmetry, it is possible that the signal is diffused or that a non-crystallographic twofold is closely aligned with a cell (screw) axis. Alternatively, the two subunits may not be identical, as was seen in the CbnR structure, albeit only in the orientation between the effector-binding domain and the DNA-binding domain (Muraoka, Okumura, Uragami *et al.*, 2003). An isomorphous selenomethionyl derivative of BenM-EBD has been prepared for MAD phasing. The CatM-EBD crystal had a single monomer per asymmetric unit, a V_M of 2.5 Å^3 Da^{-1} and a calculated solvent content of 49.5%.

The high-resolution diffraction of the BenM-EBD and CatM-EBD and effector-complex crystals suggests that the crystals make excellent candidates for structural studies. Either would represent only the fourth structure of a LysR-type transcriptional activator, despite the widespread distribution of LTTRs. By comparing the different structures with and without effectors, we may be able to characterize the synergistic response of BenM at a molecular level and relate this to the absence of such a response by CatM.

The authors wish to thank the staff at the Hauptman–Woodward Institute (http://www.hwi.buffalo.edu) for performing the high-throughput crystallization screens. The assistance of the staff at the Structural Biology Center Collaborative Access Team (SBC-CAT) 19-BM beamline at the Advanced Photon Source, Argonne National Laboratory is also gratefully acknowledged. Use of the Advanced Photon Source was supported by the US Department of Energy, Office of Science, Office of Basic Energy Sciences under Contract No. W-31-109-Eng-38. We also thank Jay Houston and Hao Xu for help collecting X-ray data and Sarah Craven, Patrick Curtis, Obidimma Ezezika and Theresa Rogers for their contributions to protein purification and crystallization optimization. Sarah Craven was supported by a grant for undergraduate research (NSF DBI-0139083). This research was supported by a grant (MCB-0212604) to EN from the National Science Foundation.

References

Brzostowicz, P. C., Reams, A. B., Clark, T. J. & Neidle, E. L. (2003). *Appl. Environ. Microbiol.* **69**, 1598–1606.
Bundy, B. M., Collier, L. S., Hoover, T. R. & Neidle, E. L. (2002). *Proc. Natl Acad. Sci. USA*, **99**, 7693–7698.
Chayen, N. E. (1997). *Structure*, **5**, 1269–1274.
Choi, H., Kim, S., Mukhopadhyay, P., Cho, S., Woo, J., Storz, G. & Ryu, S. (2001). *Cell*, **105**, 103–113.
Clark, T. J., Momany, C. & Neidle, E. L. (2002). *Microbiology*, **148**, 1213–1223.
Clark, T. J., Phillips, R. S., Bundy, B. M., Momany, C. & Neidle, E. L. (2003). Submitted.
Collaborative Computational Project, Number 4 (1994). *Acta Cryst.* D**50**, 760–763.
Collier, L. S., Gaines, G. L. III & Neidle, E. L. (1998). *J. Bacteriol.* **180**, 2493–2501.
Henikoff, S., Haughn, G. W., Calvo, J. M. & Wallace, J. C. (1988). *Proc. Natl Acad. Sci. USA*, **85**, 6602–6606.
Luft, J. R., Wolfley, J., Jusrisica, I., Glasgow, J., Fortier, S. & DeTitta, G. T. (2001). *J. Cryst. Growth*, **232**, 591–595.
Matthews, B. W. (1968). *J. Mol. Biol.* **33**, 491–497.
Muraoka, S., Okumura, R., Ogawa, N., Nonaka, T., Miyashita, K. & Senda, T. (2003). *J. Mol. Biol.* **328**, 555–566.
Muraoka, S., Okumura, R., Uragami, Y., Nonaka, T., Ogawa, N., Miyashita, K. & Senda, T. (2003). *Protein Pept. Lett.* **10**, 325–329.
Navaza, J. (1994). *Acta Cryst.* A**50**, 157–163.
Neidle, E. L., Hartnett, C. & Ornston, L. N. (1989). *J. Bacteriol.* **171**, 5410–5421.
Ogawa, N., McFall, S. M., Klem, T. J., Miyashita, K. & Chakrabarty, A. M. (1999). *J. Bacteriol.* **181**, 6697–6705.
Ogawa, N. & Miyashita, K. (1999). *Appl. Environ. Microbiol.* **65**, 724–731.
Otwinowski, Z. & Minor, W. (1997). *Methods Enzymol.* **276**, 307–326.
Quiocho, F. (1991). *Curr. Opin. Struct. Biol.* **1**, 922–933.
Romero-Arroyo, C. E., Schell, M. A., Gaines, G. L. III & Neidle, E. L. (1995). *J. Bacteriol.* **177**, 5891–5898.
Schell, M. A. (1993). *Annu. Rev. Microbiol.* **47**, 597–626.
Smith, G. D. & Dodson, G. G. (1992). *Biopolymers*, **32**, 441–445.
Tong, L. & Rossmann, M. G. (1997). *Methods Enzymol.* **276**, 594–611.
Tyrrell, R., Davies, G. J., Wilson, K. S. & Wilkinson, A. J. (1994). *J. Mol. Biol.* **235**, 1159–1161.
Tyrrell, R., Verschueren, K. H., Dodson, E. J., Murshudov, G. N., Addy, C. & Wilkinson, A. J. (1997). *Structure*, **5**, 1017–1032.
Verschueren, K. H., Addy, C., Dodson, E. J. & Wilkinson, A. J. (2001). *Acta Cryst.* D**57**, 260–262.